Original Article

MOLECULAR METABOLISM

Ghrelin transport across the blood—brain barrier can occur independently of the growth hormone secretagogue receptor

Elizabeth M. Rhea [1,2], Therese S. Salameh [1,2], Sarah Gray [3], Jingjing Niu [3], William A. Banks [1,2], Jenny Tong [3,*]

ABSTRACT

Objective: The blood—brain barrier (BBB) regulates the entry of substrates and peptides into the brain. Ghrelin is mainly produced in the stomach but exerts its actions in the central nervous system (CNS) by crossing the BBB. Once present in the CNS, ghrelin can act in the hypothalamus to regulate food intake, in the hippocampus to regulate neurogenesis, and in the olfactory bulb to regulate food-seeking behavior. The goal of this study was to determine whether the primary signaling receptor for ghrelin, the growth hormone secretagogue receptor (GHSR), mediates the transport of ghrelin from blood to brain.

Methods: We utilized the sensitive and quantitative multiple-time regression analysis technique to determine the transport rate of mouse and human acyl ghrelin (AG) and desacyl ghrelin (DAG) in wildtype and Ghsr null mice. We also measured the regional distribution of these ghrelin peptides throughout the brain. Lastly, we characterized the transport characteristics of human DAG by measuring the stability in serum and brain, saturability of transport, and the complete transfer across the brain endothelial cell.

Results: We found the transport rate across the BBB of both forms of ghrelin, AG, and DAG, were not affected by the loss of GHSR. We did find differences in the transport rate between the two isoforms, with DAG being faster than AG; this was dependent on the species of ghrelin, human being faster than mouse. Lastly, based on the ubiquitous properties of ghrelin throughout the CNS, we looked at regional distribution of ghrelin uptake and found the highest levels of uptake in the olfactory bulb.

Conclusions: The data presented here suggest that ghrelin transport can occur independently of the GHSR, and ghrelin uptake varies regionally throughout the brain. These findings better our understanding of the gut-brain communication and may lead to new understandings of ghrelin physiology.

Keywords Ghrelin; Blood—brain barrier; Growth hormone secretagogue receptor; Pharmacokinetics

1. INTRODUCTION

Ghrelin is a 28-amino acid peptide mainly produced in the stomach and small intestines with the kidneys, placenta, and pancreas contributing to miniscule amounts of circuiting ghrelin [1]. Ghrelin exists in circulation in two major forms: acyl ghrelin (AG) and desacyl ghrelin (DAG). During posttranslational processing, proghrelin is coupled with an octanoic acid at the serine-3 residue by the membrane-bound enzyme, ghrelin O-acyltransferase (GOAT), to form AG [2,3]. This fatty acid modification is entirely unique to ghrelin and is required for the optimal binding of ghrelin to its receptor, the growth hormone secretagogue receptor (GHSR) 1a [4,5], which is a 7-transmembrane G-protein coupled receptor widely expressed in body tissues but with the highest expression in the CNS (i.e. pituitary gland) [5,6]. AG acts peripherally and centrally to regulate biological functions including stimulating growth hormone secretion, promoting positive energy balance and food reward, regulating glucose metabolism, and enhancing gut motility [7]. DAG is the predominant form of ghrelin, but the lack of acylation precludes it from binding to GHSR 1a and subsequent receptor activation [1,8]. Despite this, many biological functions have been ascribed to DAG, including the protective effect of cortical neuronal injury, regulation of glucose and lipid metabolism, food intake, and stress behavior [9—14]. We have shown previously that ghrelin also enhances sniffing and olfactory sensitivity, two important functions for food seeking, by acting directly on the olfactory bulb [15].

It has been long recognized that in the brain, particularly in the hypothalamus, ghrelin plays a key role in the homeostatic regulation of energy and glucose metabolism [10,16,17]. Additionally, ghrelin may modulate reward neurocircuits and memory by acting in areas of the brain behind an intact blood—brain barrier (BBB) [7]. Nutrients and signals from the gut, pancreas, and adipose tissue are transported to

[1]VA Puget Sound Health Care System, Seattle, WA, USA [2]Division of Gerontology and Geriatric Medicine, Department of Medicine, University of Washington, Seattle, WA, USA [3]Division of Endocrinology, Metabolism, and Nutrition, Duke Molecular Physiology Institute, Department of Medicine, Duke University, Durham, NC, USA

*Corresponding author. E-mail: jenny.tong@duke.edu (J. Tong).

Abbreviations: GHSR, Growth hormone secretagogue receptor; mAG, mouse acyl ghrelin; hAG, human acyl ghrelin; mDAG, mouse des acyl ghrelin; hDAG, human des acyl ghrelin; GI, gastrointestinal (GI)

Received August 3, 2018 • Revision received September 10, 2018 • Accepted September 18, 2018 • Available online 24 September 2018

https://doi.org/10.1016/j.molmet.2018.09.007

the central nervous system (CNS) by crossing the BBB or the blood-cerebrospinal fluid (CSF) barrier [18,19]. To cross the vascular BBB, substances must cross the restrictive brain endothelium and then traverse astrocyte endfeet before reaching brain interstitium [20]. We and others have shown that the BBB plays a direct role in mediating communication between the brain and the gastrointestinal (GI) tract by controlling the transfer of peptides and regulatory proteins between blood and CNS [21]. Not only can the GI tract secrete substances that affect CNS function [22,23], but GI hormones can modulate brain endothelial cells and alter their ability to secret substances into the CNS affecting behavior or function [24,25]. An example of such gut-brain communication is the orexigenic effect of ghrelin. The stomach derived hormone works centrally by activating the neuropeptide Y/agouti-related protein (NPY/AgRP) neurons and inhibiting the pro-opiomelanocortin (POMC) neurons in the hypothalamus to promote a positive energy balance [26–28].

We previously studied the ability of human AG (hAG), mouse AG (mAG), and mouse DAG (mDAG) to cross the BBB of the mouse brain in the brain-to-blood and blood-to-brain directions and found that AG (mouse and human) crosses the BBB in a bidirectional and saturable manner, but mDAG only travels from blood to brain unidirectionally and in an unsaturable manner [29]. These paradoxical findings suggest that the transport efficiency of ghrelin may be related to the n-octanoyl side chain. The objective of the current research is to investigate whether AG transport across the BBB is GHSR dependent by using the Ghsr null mouse model. In addition, since the transport of human DAG (hDAG) across the BBB has not been previously characterized, we wanted to test its BBB transport properties to determine if hDAG transport is more efficient than hAG or mDAG. Given the known central action of ghrelin to regulate food intake and food reward, we also examined brain regional transport of ghrelin to see if the pattern correlates with its known functions.

2. MATERIALS AND METHODS

2.1. Animals

Generation and characterization of Ghsr null mice has been described previously [30]. Three to six-month old males and females were used for all studies. Mice had *ad libitum* access to food and water and kept on a 12/12 h light/dark cycle. All studies were conducted in the afternoon (~1PM). All mice were anesthetized with 0.15 mL of 40% urethane injected intraperitoneal prior to experimentation. The right jugular vein was exposed to allow for intravenous (IV) injection of each solution. The Institutional Animal Care and Use Committee at the Veterans Affairs Puget Sound (Seattle, WA) approved all animal experimental protocols, and all methods were carried out in accordance with the approved guidelines and regulations. The VA Puget Sound is a facility that is certified by the Association for Assessment and Accreditation of Laboratory Animal Care International.

2.2. Radioactive labeling

The synthetic ghrelin peptides (CSBio, Inc, Menlo Park, CA) were radioactively labeled as follows. Ten micrograms of each peptide was labeled with 1.0 mCi sodium ^{125}I (Perkin Elmer, Waltham, MA) by addition of 10 μg of chloramine-T (Sigma–Aldrich, St. Louis, MO) in 0.25 M chloride-free sodium phosphate buffer, pH 7.5. After 1 min, the reaction was terminated by adding 100 μg of sodium metabisulfite. Albumin (Sigma–Aldrich, St. Louis, MO) was labeled with 1.0 mCi ^{99m}Tc (GE Healthcare, Seattle, WA) by combining 1 mg albumin with 120 μg stannous tartrate and 20 μL 1M HCl in 500 µL deionized water for 20 min. Radioactively labeled ghrelins (^{125}I-ghrelin) and albumin (^{99m}Tc-Alb) were purified on Sephadex G-10 columns (Sigma–Aldrich). Protein labeling by iodine or by technetium isotopes was characterized by 30% trichloroacetic acid (TCA) precipitation for albumin and AGs while acidified brine was used to precipitate the DAGs. Greater than 90% radioactivity in the precipitated fraction was consistently observed for the ghrelin peptides and albumin.

2.3. Measurement of brain influx and initial volume of distribution in brain

Multiple-time point regression analysis was used to calculate the blood-to-brain unidirectional influx rate (K_i) as previously described [31,32]. Following anesthetization, mice were administered 0.2 mL of 1% bovine serum albumin in lactated Ringer's solution (1% BSA/LR) containing 1×10^6 cpm of a ^{125}I-ghrelin peptide and 5×10^5 cpm of ^{99m}Tc-Alb into the jugular vein. The specific activity for each ^{125}I-ghrelin peptide is 25 Ci/g, which equals approximately 20 ng per dose of 1×10^6 cpm ^{125}I-ghrelin peptide. Blood from the carotid artery was collected between 1 and 10 min after the IV injection. Immediately after the blood draw, mice were decapitated, and brains were removed and weighed. The arterial blood was centrifuged at 3200 g for 10 min at 4 °C, and the serum was collected. Levels of radioactivity in serum (50 µL) and brain were counted in a gamma counter for 3 min and recorded as counts per minute (cpm). The brain/serum (B/S) ratios (µL/g) of the ^{125}I-ghrelin in each gram of brain were calculated separately and were plotted against their respective exposure times, which were calculated using the following formulas derived from Patlak and Blasberg [31,32]:

$$\frac{Am}{Cpt} = Ki\left(\frac{\int_0^t Cp(t)dt}{Cp(t)}\right) + Vi \quad (1)$$

where Am is the level of radioactivity (cpm) per g of brain, Cp is the level of radioactivity (cpm) in arterial serum at time *t*, and exposure time in minutes is measured by the term

$$\frac{\int_0^t Cp(t)dt}{Cp(t)} \quad (2)$$

The linear portion of the relation between the B/S ratios and exposure time was used to calculate K_i (µL/g-min) and V_i (µL/g), the initial volume of distribution in brain at t = 0, which is defined as the functional volume per unit brain mass of a soluble compound that exchanges rapidly and reversibly with plasma [31]. The slope of the linear portion of the relationship between B/S ratios and exposure time defines K_i and is reported with its error term. The y-intercept of this linear portion of the relationship defines V_i.

2.4. *In vivo* stability of ^{125}I- hDAG in brain and blood

^{125}I-hDAG containing 1×10^6 cpm in 0.2 mL of 1% BSA/LR solution was injected IV and allowed to circulate for 2, 6, and 10 min. Blood and whole brain were collected. The blood was centrifuged at 3200 g for 10 min and 50 µL of the resulting serum added to 250 µL of 1% BSA/LR. After vortexing, 300 µL of acidified brine was added to it, vortexed again, and then centrifuged for 10 min at 5400 g. The radioactivity in the resulting supernatant (S) and precipitate (P) was counted separately, and the percent cpm in the precipitate was calculated (% Precip). Brains were homogenized in 0.8 mL of 1% BSA/LR using a bead beater for 30 s at 4800 rpm twice. Samples were transferred to a 1.7 mL microfuge tube and centrifuged at 5400 g for 10 min and a portion of the resulting supernatant added to an equal volume of

acidified brine, vortexed, and centrifuged at 5400 g for 10 min. The radioactivity in the resulting S and P fractions were counted separately, and the % Precip calculated as above.
To correct for any degradation that might have occurred during the acid precipitation processing, ^{125}I-hDAG was added *ex vivo* to non-radioactive blood or to whole brain and processed as above. Biological samples were corrected for degradation during processing by dividing their values by the processing control values. The values for % Precip from the biological samples was corrected by dividing them by the % Precip values for the processing controls and multiplying by 100 to yield the corrected value.

2.5. Complete transfer of ^{125}I-hDAG across the brain endothelial cell

The capillary depletion method was used to determine whether the ^{125}I-hDAG completely crossed the capillary wall to enter brain by separating cerebral capillaries from brain parenchyma. Mice received an IV injection of 1×10^6 cpm of ^{125}I-hDAG with 5×10^5 cpm ^{99m}Tc-Alb in 0.2 mL 1% BSA/LR. Ten min later, blood was collected from the carotid artery, and the brains were removed. Whole brains were homogenized in glass with 0.8 mL physiological buffer (10 mM HEPES, 141 mM NaCl, 4 mM KCl, 2.8 mM $CaCl_2$, 1 mM $MgSO_4$, 1 mM NaH_2PO_4, 10 mM D-glucose, pH 7.4) and mixed thoroughly with 1.6 mL 26% dextran in the same physiological buffer. The homogenate was centrifuged at 5400 g for 15 min at 4 °C. The capillary-containing pellet and the supernatant, representing the brain parenchymal/interstitial fluid space, were carefully separated. The ratio of ^{125}I-hDAG radioactivity in the supernatant (parenchyma) was corrected for vascular space by subtracting the ratio of ^{99m}Tc-Alb in the supernatant. The parenchyma/serum and capillary/serum ratios (μL/g) were calculated by the equation:

$$\text{Ratio} = (\text{cpm/g of tissue})/(\text{cpm/}\mu\text{L of serum}) \quad (3)$$

2.6. Competitive transport of ^{125}I-hDAG

To determine whether brain uptake of ^{125}I-hDAG was saturable, 1 and 10 μg/mouse non-radioactive hDAG was included in the IV injection of some mice. Blood was collected from the left carotid artery, and the whole brain was removed and weighed 10 min after IV injection of 1×10^6 cpm of ^{125}I-hDAG with 5×10^5 cpm of ^{99m}Tc-Alb in 0.2 mL 1% BSA/LR. Results are expressed as B/S ratios (μL/g) after correction for the amount of vascular space.

2.7. Regional distribution

Ten min after 0.2 mL IV injection of the radiolabeled solution containing 1×10^6 cpm of ^{125}I-ghrelin peptides with 5×10^5 cpm of ^{99m}Tc-Alb, blood was collected and brains were removed. Brains were dissected on ice into the olfactory bulb, 10 brain regions according to Glowinski and Iversen [33] and then the cortices combined to represent the cortex. Radioactive values were corrected for vascular space as described above and are expressed as tissue/serum ratios (μL/g). Abbreviations are as follows: whole brain (WB), olfactory bulb (OB), cortex (Ctx), striatum (Str), hypothalamus (Hypo), hippocampus (Hippo), thalamus (Thal), cerebellum (CB), midbrain (Mid), pons (Pons).

2.8. Statistics

Regression analysis and other statistical analyses were performed with the use of Prism 6.0 (GraphPad Software Inc., San Diego, CA, USA). Linear regression lines are reported with their correlation coefficients (r) and *p* values. To determine whether entry rates into brain differ, two or more regression lines can be compared using the statistical package in Prism. Normality of residuals for the linear regression was tested by the Shapiro—Wilk Test and all passed this normal distribution test. Transport characteristics of hDAG were compared by a one-way analysis of variance (ANOVA). Brain region data were compared by two-way ANOVA followed by Sidak's multiple comparison post-test. All other data where necessary is reported as the mean with the standard error terms.

3. RESULTS

3.1. Brain influx and initial volume of distribution after intravenous injection

Figure 1 is a graphical representation of the rates of brain influx for all the ghrelin peptides completed in wildtype (WT) and Ghsr null mice. A significant blood-to-brain unidirectional influx rate was measurable for all of the ^{125}I-ghrelin peptides examined. Table 1 lists the K_i and V_i measured for each ghrelin peptide. As shown in Table 1, hDAG had the fastest influx rate in the WT (0.7944 ± 0.10 μL/g • min, $r = 0.959$, $p < 0.001$; $n = 10$ mice/time curve) and Ghsr null (0.6448 ± 0.07 μL/g • min, $r = 0.950$, $p < 0.001$; $n = 9$ mice/time curve) animals. Mouse AG had the slowest measurable influx rate in the WT mice (0.1852 ± 0.06 μL/g • min, $r = 0.758$, $p = 0.018$; $n = 10$ mice/time curve). Mouse DAG had the slowest measurable influx rate in the Gshr null mice (0.2032 ± 0.05 μL/g • min, $r = 0.782$, $p = 0.004$; $n = 6$ mice/time curve). No significant difference was detected in brain influx rate between WT and Ghsr null mice among each of the ghrelin peptides tested. The initial volume of distribution (V_i) in the brain ranged from 1.192 ± 0.5740 μL/g in the WT hAG to 3.102 μL/g $\pm$ 0.41 in the Ghsr null mDAG; V_i for the other ghrelin peptides are listed in Table 1. Human DAG showed a significant difference in the V_i between WT (1.775 ± 0.81 μL/g • min) and Ghsr null mice (1.555 ± 0.67 μL/g • min). No ^{99m}Tc-Alb uptake was observed during this period (data not shown).

3.2. ^{125}I-hDAG transport characterization

After measuring the transport rate of all ghrelins across the BBB, we wanted to further investigate the transport properties of hDAG as this peptide has not been previously characterized. The amount of degradation in serum and brain was measured by acid precipitation of radioactivity recovered from these samples. Serum levels did not fall below 100% (Figure 2A). In the latest time point studied, 10 min, greater than 60% of the radioactivity recovered from the brain was precipitated by acid. Therefore, we can conclude the level of ^{125}I-hDAG present in brain appeared after intact transport across the BBB as the peptide is intact in the serum at this latest time point.
In order to determine whether ^{125}I-hDAG was able to completely transport across the brain endothelial cell, we separated the capillaries from the brain parenchyma 10 min after circulation and measured radioactivity present in these fractions. Indeed, the majority of the ^{125}I-hDAG was present in the parenchyma (10.4 ± 1.95 μL/g) compared to the capillary fraction (1.0 ± 0.30 μL/g) (Figure 2B).
The uptake for brain ^{125}I-hDAG was not saturable at two different doses of unlabeled hDAG (1 μg and 10 μg) 10 min after circulation (Figure 2C).

3.3. Regional ghrelin distribution

To determine if the brain distribution of the ghrelin peptides varied between WT and Ghsr null mice, we measured regional levels of each ^{125}I-ghrelin 10 min after IV injection (Figure 3). For all ghrelins, there were significant differences within each genotype for brain regions ($p < 0.0001$) with the olfactory bulb and pons containing the greatest

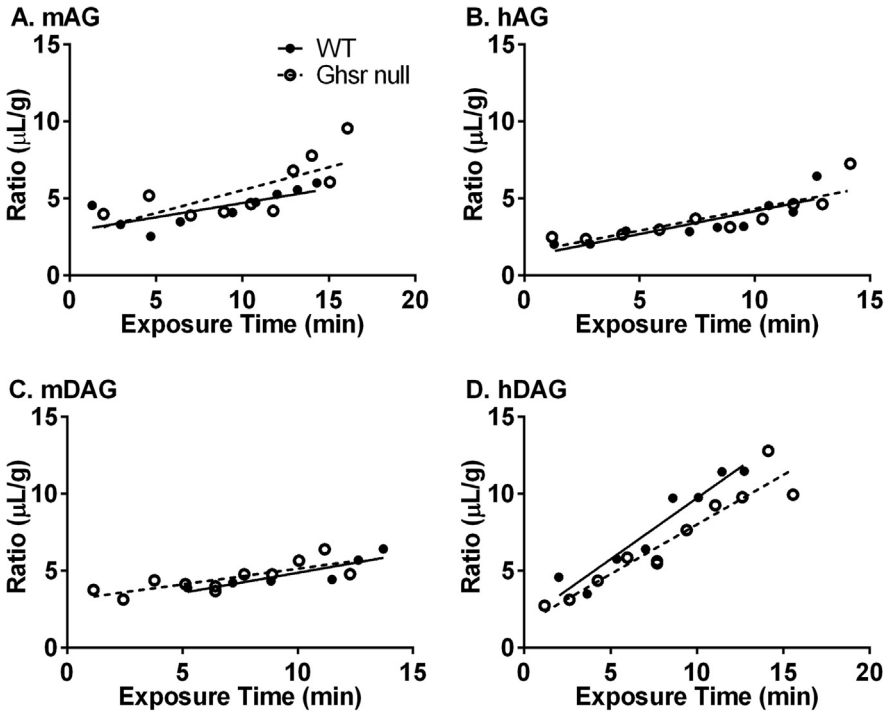

Figure 1: Blood-to-brain influx of ^{125}I-ghrelin peptides in WT and Ghsr null mice. No significant difference in A) mAG, B) hAG, C) mDAG, or D) hDAG influx was observed between WT (closed circles, n = 10–11) and Ghsr null mice (open circles, n = 6–9).

Table 1 — Pharmacokinetics of ghrelin transport into the whole brain.

Ghrelin Peptide	Genotype	K_i (μL/g-min)	r	p	V_i (μL/g)
mAG	WT	0.1852 ± 0.06	0.758	0.018	2.847 ± 0.57
	Ghsr null	0.2976 ± 0.10	0.722	0.018	2.560 ± 1.12
hAG	WT	0.2979 ± 0.07	0.858	0.003	1.192 ± 0.57
	Ghsr null	0.2853 ± 0.06	0.856	0.002	1.478 ± 0.55
mDAG	WT	0.2606 ± 0.07	0.872	0.024	2.265 ± 0.75
	Ghsr null	0.2032 ± 0.05	0.783	0.004	3.102 ± 0.41
hDAG	WT	0.7944 ± 0.10	0.959	<0.001	1.775 ± 0.81*
	Ghsr null	0.6448 ± 0.07	0.950	<0.001	1.555 ± 0.67*

Levels of ^{125}I-ghrelin (mAG, hAG, mDAG, and hDAG) present in whole brain in WT and Ghsr null mice were measured 1–10 min after injection and plotted in Figure 1. Multiple-time point regression analysis was performed to determine the rate of ghrelin transport (K_i) and vascular binding (V_i). Data are presented as mean ± SEM. *p < 0.05 between WT and Ghsr null for hDAG.

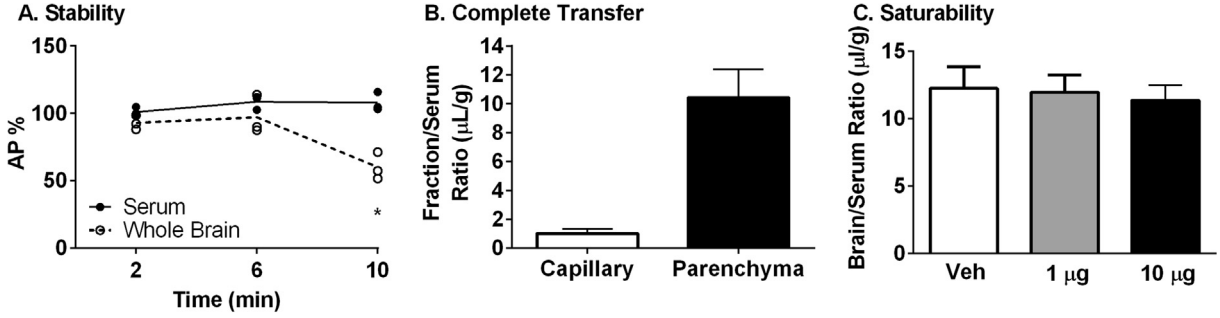

Figure 2: Characterization of ^{125}I-hDAG. A) Stability in serum and whole brain (Whole Brain *p < 0.05 vs 2 and 6 min). B) Complete transfer across the brain endothelial cell (n = 3). C) Lack of saturable transport (One-Way ANOVA: p = 0.89, n = 9).

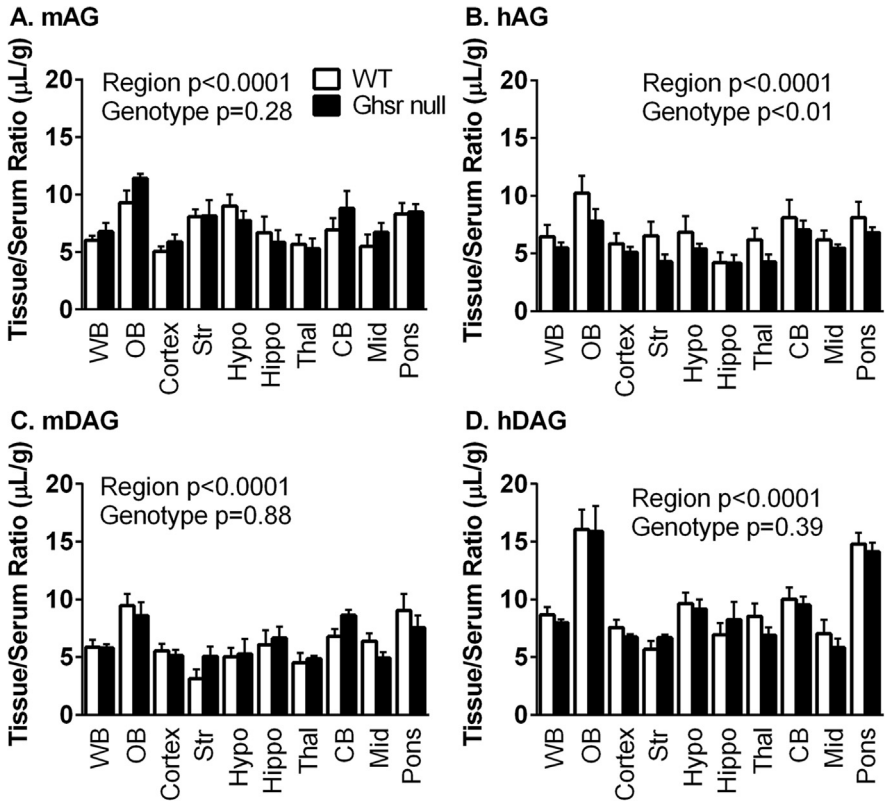

Figure 3: Regional distribution of ghrelin peptides. Levels of ^{125}I-ghrelin peptides were measured in each brain region after 10 min circulation. There were significant differences in the regional distribution of A) mAG, B) hAG, C) mDAG, and D) hDAG levels. There was also a difference due to genotype with B) hAG. (n = 5–7 per region per genotype).

levels. Using a two-way ANOVA, the only peptide that showed significant differences due to genotype was hAG ($p = 0.0025$) with 7.68% of total variation (Figure 3B). There were no individual differences in the post-hoc analysis. The mean ± SEM of each ^{125}I-ghrelin present in each brain region is listed in Table 2 with more detailed statistical information regarding brain region differences. Figure 4 represents the brain distribution using a heat map of the cumulative data. Data were collapsed for the ghrelin peptides where there was no difference due to genotype (mAG, mDAG, hDAG). For hAG, data were represented for both WT (Figure 4D) and Ghsr null (Figure 4E) mice.

4. DISCUSSION

The highly-restrictive BBB is the paramount obstacle for the entry of circulating substances into brain tissue and plays a direct role in mediating the communication between the brain and the GI tract. In this study, we have characterized the transport of mouse and human AG and DAG in WT and Ghsr null mice. The data presented here suggest transport of ghrelin across the BBB in either the AG or DAG form does not require the GHSR. However, we did observe differences in the transport efficiency between the two isoforms, dependent on species: mouse or human. We found hDAG was transported faster than the other peptides: mDAG, mAG, and hAG. As hDAG BBB transport has not been characterized previously, we found this peptide was stable in serum, completely transferred across the BBB, and transport was not saturable at the doses tested. Lastly, we found all forms of exogenous ghrelin were regionally distributed throughout the brain, collecting primarily in the olfactory bulb and pons-medulla. Loss of GHSR only resulted in significant differences in hAG accumulation throughout the brain.

Several peripheral hormones that are involved in the central regulation of energy homeostasis, such as leptin, insulin, and amylin [34–38], cross the BBB by saturable and unsaturable mechanisms. Whether these transport processes are predominantly by signaling receptor-mediated transport is debated. A novel aspect of this study was to determine whether the GHSR mediated transfer of ghrelin from blood to brain. To test this, we compared the transport rate of the human and mouse ghrelin forms in WT mice and Ghsr null mice. We found the transport rate across the BBB did not differ with the loss of GHSR. This suggests the signaling-related receptor for ghrelin is not the ghrelin transporter. This is not the first time it has been shown a peptide is transported via a different protein than the canonical signaling receptor. For example, the efflux transporter for PACAP27, a pluripotent neuropeptide, is β-F1 ATPase, a component of peptide transport system-6, and differs from the canonical signaling-related receptors, PAC1, VPAC1, and VPAC2 [39]. In addition, epidermal growth factor transporters differ from their signaling-related receptor [40].

There is consensus in the field that ghrelin is not synthesized in the brain [41,42]. Therefore, the orexigenic actions of ghrelin depend on the ability of peripheral ghrelin to assess the neuronal circuits of food intake regulation. Ghrelin can gain access to the brain through the circumventricular organs (CVOs), blood-cerebrospinal fluid barrier, and the BBB [43]. We focused our research on ghrelin transport through the BBB and found that, under *ad lib* fed conditions, radioactive mAG has low accessibility to the mouse brain and the levels in the hypothalamus were similar to the cortex, thalamus, and whole brain. These findings raise questions about the physiologic importance of the peripheral AG transported across the BBB to reach its central targets. However, there is evidence for fasting to enhance peripheral metabolic signaling to the

Table 2 — Regional distribution of ^{125}I-ghrelins in WT and Ghsr null mice.

		mAG				hAG				mDAG				hDAG			
		WT		Ghsr Null		WT		Ghsr Null		WT		Ghsr Null		WT		Ghsr Null	
Brain Region	Abbreviation	Mean	SEM	Mean	SEM	Mean	SEM	Mean	SEM	Mean	SEM	Mean	SEM	Mean	SEM	Mean	SEM
Whole Brain	WB	6.01	0.414	6.77	0.766	6.45	1.02	5.48	0.458	5.86	0.646	5.79	0.324	8.67	0.674	7.98	0.289
Olfactory Bulb	OB	9.31	1.044	11.43	0.399	10.2	1.49	7.79	1.07	9.46	1.01	8.57	1.19	16.1	1.74	15.9	2.22
Cortex	Ctx	5.06	0.409	5.89	0.642	5.84	0.904	5.11	0.464	5.55	0.619	5.15	0.476	7.56	0.662	6.75	0.246
Striatum	Str	8.05	0.678	8.16	1.37	6.52	1.22	4.3	0.628	3.14	0.802	5.07	0.841	5.67	0.725	6.67	0.264
Hypothalamus	Hypo	9.00	0.995	7.74	0.854	6.83	1.41	5.39	0.458	5.02	0.79	5.27	1.29	9.62	0.948	9.16	0.806
Hippocampus	Hippo	6.69	1.422	5.85	1.083	4.19	0.906	4.17	0.702	6.08	1.26	6.64	0.998	6.92	1.03	8.25	1.55
Thalamus	Thal	5.67	0.797	5.29	0.902	6.17	1.04	4.27	0.644	4.53	0.811	4.85	0.257	8.53	1.11	6.89	0.686
Cerebellum	CB	6.93	1.008	8.81	1.511	8.09	1.56	7.03	0.818	6.77	0.66	8.62	0.477	10	1.01	9.51	0.73
Midbrain	Mid	5.49	1.045	6.71	0.840	6.16	0.834	5.46	0.294	6.37	0.687	4.91	0.53	7.02	1.22	5.82	0.792
Pons-Medulla	Pons	8.33	0.939	8.50	0.661	8.09	1.37	6.8	0.465	9.04	1.44	7.54	1.05	14.8	0.965	14.1	0.791

Data are represented in Figure 3 but reported here as mean with SEM (n = 5—7/brain region). Two-Way ANOVA shows a significant effect of regional distribution for each peptide: hDAG $p < 0.0001$ WT (WB different from OB, Pons; OB different from all regions; Pons different from all regions) and Ghsr Null (WB different from OB, Pons; OB different from all regions; Pons different from all regions except Mid); mDAG $p < 0.0001$ WT (OB different from Str, Hypo, Thal; Pons different from Str, Thal); hAG $p = 0.0011$ WT (no post-hoc differences); mAG $p < 0.0001$ Ghsr Null (OB different from Ctx, Hippo, Thal, Mid).

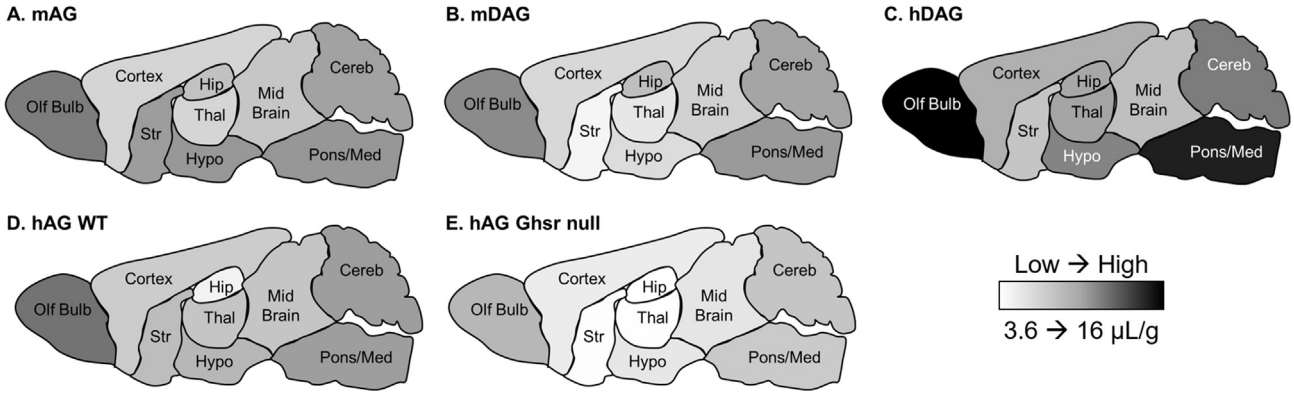

Figure 4: Pictorial representation of ^{125}I-ghrelins brain distribution. A heat map was generated based on the data in Table 2. A—C) Data are collapsed across genotype. D—E) Data are separated for ^{125}I-hAG due to statistically significant differences between genotypes.

arcuate nucleus of the hypothalamus (ARH) [44], and we have shown enhanced BBB transport of human AG into whole brain [21]. Our previous studies also showed a numerical increase in hAG entry into whole brain in 48-hr starved mice, compared to fed mice; however, this was not statistically significant [21]. We did not examine ghrelin-mediated signaling in neurons in this study, but it is curious whether fasting would increase the BBB transport of ghrelin into the ARH and whether AG and DAG would be affected similarly. While our studies involved large, regional dissections, other studies have investigated more detailed entry into sub-regions [45], especially in the hypothalamus, and found differences in transport within this brain region. AG was able to rapidly access neurons of the ARH near fenestrated capillaries in the median eminence [45]. However, the precise transport mechanism for ghrelin into these regions has yet to be determined.

Various forms of ghrelin (hAG, mAG, and mDAG) have been previously investigated in terms of BBB transport and characteristics [29]. We found the same pattern of transport rate with mDAG > hAG > mAG in the current study. Additionally, we also investigated the transport rate of hDAG in comparison to the other ghrelin forms as there are multiple CNS biological functions attributed to DAG despite its inability to activate the GHSR. Surprisingly, we found hDAG was transported approximately three times faster than the other three forms. Therefore, the new hierarchy of transport is hDAG > mDAG > hAG > mAG in mice. It should be noted, our study included males and females combined in determining the transport rate for each ghrelin peptide. Therefore, further studies should investigate a potential sexual dimorphism in the transport of ghrelin across the BBB. Human and mouse AG only differ in sequence at amino acids 11—12 [46], and human and mouse GHSR are 95% identical. To our knowledge, the binding affinity of human ghrelins to mouse GHSR and vice versa has not been addressed. The slower transport of AG could be due to the presence of its octanoyl group since the octanoyl tail allows it to circulate bound to HDL, LDL, and triglyceride-rich lipoproteins, while DAG only binds to HDL [47,48]. It is also possible the brain-to-blood efflux system for ^{125}I-AG contributes to the slower overall transport rate [29].

We have previously shown in the same time frame reported here (10 min) that AG was not degraded into DAG [29] and that the half-life of AG in human serum is ~10 min [49]. However, we cannot rule out in this study that there is not breakdown to DAG that could contribute to the levels of ^{125}I-ghrelin measured in brain. AG breakdown to DAG can be done by numerous circulating esterases, including butylcholinesterase and carboxypeptidase, and it is possible for various esterases to compensate when one is lacking [50]. However, what contributes to the further breakdown of DAG in brain is not known. Whether hAG and mAG are hydrolyzed at different rates in our mice is unknown and may provide another mechanism for the differences we have detected in transport.

To gain insight into brain regions that are involved in the central action of ghrelin, we determined the regional transport of the ghrelin peptides

throughout the brain. While the overall accumulation of each ghrelin peptide varies for the brain regions, there is a significant difference in regional accumulation with greater levels present in the hypothalamus compared to the hippocampus and cortex. The differences in peptide accumulation for each brain region are likely due to recognition of the isoform with the transporter. The brain region with the highest level of each ghrelin peptide, regardless of species, was the olfactory bulb. We previously reported that the GHSR1a is present in olfactory circuits in the brain; ghrelin enhances food-seeking behavior by stimulating exploratory sniffing and increasing olfaction sensitivity [15]. Our finding is similar to the previous report by Diano et al. that the olfactory bulb (along with occipital cortex) exhibits the highest uptake of peripherally injected radiolabeled human ghrelin in the mouse brain [51]. We are unaware whether fasting induces changes of ghrelin transport specific to the olfactory bulb. If long-term fasting is altering the structure of the BBB or c-Fos expression, ghrelin transport could also be altered. For most ghrelin forms, there was no effect of genotype on regional distribution. However, for hAG, there was a significant effect of genotype; the Ghsr null mice had consistently lower levels in each brain region compared to WT. Since only a single time point was taken to collect these data, we cannot determine if the decreased level is due to a decrease in binding to the GHSR, altered efflux, or overall transport. Based on the finding that hDAG BBB transport rate is greater than the other previously characterized ghrelin forms, we wanted to further characterize the transport characteristics of hDAG. We found hDAG was intact in mouse serum yet brain hDAG was ~60% intact by 10 min. We also observed nearly complete transfer of hDAG across the brain endothelial cell and into the brain parenchyma. Lastly, we investigated the saturability of hDAG transport. At two different doses of unlabeled hDAG, 1 μg and 10 μg, the amount of ^{125}I-hDAG present in the brain was not statistically different. These data suggest this system is not saturable at these doses. These results are similar to the data reported previously [29].

5. CONCLUSIONS

In conclusion, our results show for the first time the GHSR is not solely responsible for ghrelin transport across the BBB. At this time, it is unclear whether the two forms (AG and DAG) are transported by the same protein. In addition, we show ghrelin levels are highest in the olfactory bulb, regardless of the form of ghrelin. We also newly characterized hDAG transport characteristics in addition to comparing the results from mDAG, hAG, and mAG BBB transport to previously reported literature [29]. Both human and mouse DAGs are transported faster across the BBB compared to AG while human ghrelin peptides are transported more efficiently than mouse ghrelin. The information gained from these results aid in better understanding the gut-brain communication and provide new foundations for future investigations to connect these findings with physiological functions of ghrelin.

FUNDING

This work was supported by the National Institutes of Health (RO1DK097550 to JT, RO1AG046619 to WAB and TS, and T32AG000057 to EMR, and T32DK007012 to SG) and by the Veterans Affairs Puget Sound Health Care System Research and Development.

CONFLICT OF INTEREST

None.

REFERENCES

[1] Kojima, M., Hosoda, H., Date, Y., Nakazato, M., Matsuo, H., Kangawa, K., 1999. Ghrelin is a growth-hormone-releasing acylated peptide from stomach. Nature 402(6762):656–660. https://doi.org/10.1038/45230 [published Online First: Epub Date].

[2] Yang, J., Zhao, T.J., Goldstein, J.L., Brown, M.S., 2008. Inhibition of ghrelin O-acyltransferase (GOAT) by octanoylated pentapeptides. Proceedings of the National Academy of Sciences of the U S A 105(31):10750–10755. https://doi.org/10.1073/pnas.0805353105 [published Online First: Epub Date].

[3] Gutierrez, J.A., Solenberg, P.J., Perkins, D.R., Willency, J.A., Knierman, M.D., Jin, Z., et al., 2008. Ghrelin octanoylation mediated by an orphan lipid transferase. Proceedings of the National Academy of Sciences of the U S A 105(17):6320–6325. https://doi.org/10.1073/pnas.0800708105 [published Online First: Epub Date].

[4] Hosoda, H., Kojima, M., Matsuo, H., Kangawa, K., 2000. Ghrelin and des-acyl ghrelin: two major forms of rat ghrelin peptide in gastrointestinal tissue. Biochemical and Biophysical Research Communications 279(3):909–913. https://doi.org/10.1006/bbrc.2000.4039 [published Online First: Epub Date].

[5] Holst, B., Cygankiewicz, A., Jensen, T.H., Ankersen, M., Schwartz, T.W., 2003. High constitutive signaling of the ghrelin receptor–identification of a potent inverse agonist. Molecular Endocrinology 17(11):2201–2210. https://doi.org/10.1210/me.2003-0069 [published Online First: Epub Date].

[6] Zigman, J.M., Jones, J.E., Lee, C.E., Saper, C.B., Elmquist, J.K., 2006. Expression of ghrelin receptor mRNA in the rat and the mouse brain. The Journal of Comparative Neurology 494(3):528–548. https://doi.org/10.1002/cne.20823 [published Online First: Epub Date].

[7] Muller, T.D., Nogueiras, R., Andermann, M.L., Andrews, Z.B., Anker, S.D., Argente, J., et al., 2015. Ghrelin. Molecular Metabolism 4(6):437–460. https://doi.org/10.1016/j.molmet.2015.03.005 [published Online First: Epub Date].

[8] Bednarek, M.A., Feighner, S.D., Pong, S.S., McKee, K.K., Hreniuk, D.L., Silva, M.V., et al., 2000. Structure-function studies on the new growth hormone-releasing peptide, ghrelin: minimal sequence of ghrelin necessary for activation of growth hormone secretagogue receptor 1a. Journal of Medicinal Chemistry 43(23):4370–4376.

[9] Chung, H., Seo, S., Moon, M., Park, S., 2008. Phosphatidylinositol-3-kinase/Akt/glycogen synthase kinase-3 beta and ERK1/2 pathways mediate protective effects of acylated and unacylated ghrelin against oxygen-glucose deprivation-induced apoptosis in primary rat cortical neuronal cells. Journal of Endocrinology 198(3):511–521. https://doi.org/10.1677/JOE-08-0160 [published Online First: Epub Date].

[10] Heppner, K.M., Piechowski, C.L., Muller, A., Ottaway, N., Sisley, S., Smiley, D.L., et al., 2014. Both acyl and des-acyl ghrelin regulate adiposity and glucose metabolism via central nervous system ghrelin receptors. Diabetes 63(1):122–131. https://doi.org/10.2337/db13-0414 [published Online First: Epub Date].

[11] Delhanty, P.J., Huisman, M., Baldeon-Rojas, L.Y., van den Berge, I., Grefhorst, A., Abribat, T., et al., 2013. Des-acyl ghrelin analogs prevent high-fat-diet-induced dysregulation of glucose homeostasis. The FASEB Journal 27(4):1690–1700. https://doi.org/10.1096/fj.12-221143 [published Online First: Epub Date].

[12] Mahbod, P., Smith, E.P., Fitzgerald, M.E., Morano, R.L., Packard, B.A., Ghosal, S., et al., 2018. Desacyl ghrelin decreases anxiety-like behavior in male mice. Endocrinology 159(1):388–399. https://doi.org/10.1210/en.2017-00540 [published Online First: Epub Date].

[13] Stark, R., Santos, V.V., Geenen, B., Cabral, A., Dinan, T., Bayliss, J.A., et al., 2016. Des-acyl ghrelin and ghrelin O-acyltransferase regulate hypothalamic-pituitary-adrenal Axis activation and anxiety in response to acute stress. Endocrinology 157(10):3946–3957. https://doi.org/10.1210/en.2016-1306 [published Online First: Epub Date].

[14] Dieguez, C., Vazquez, M.J., Romero, A., Lopez, M., Nogueiras, R., 2011. Hypothalamic control of lipid metabolism: focus on leptin, ghrelin and melanocortins. Neuroendocrinology 94(1):1—11. https://doi.org/10.1159/000328122 [published Online First: Epub Date].

[15] Tong, J., Mannea, E., Aime, P., Pfluger, P.T., Yi, C.X., Castaneda, T.R., et al., 2011. Ghrelin enhances olfactory sensitivity and exploratory sniffing in rodents and humans. Journal of Neuroscience 31(15):5841—5846. https://doi.org/10.1523/JNEUROSCI.5680-10.2011 [published Online First: Epub Date].

[16] Cowley, M.A., Smith, R.G., Diano, S., Tschop, M., Pronchuk, N., Grove, K.L., et al., 2003. The distribution and mechanism of action of ghrelin in the CNS demonstrates a novel hypothalamic circuit regulating energy homeostasis. Neuron 37(4):649—661.

[17] Andrews, Z.B., 2011. Central mechanisms involved in the orexigenic actions of ghrelin. Peptides 32(11):2248—2255. https://doi.org/10.1016/j.peptides.2011.05.014 [published Online First: Epub Date].

[18] Engelhardt, B., Sorokin, L., 2009. The blood-brain and the blood-cerebrospinal fluid barriers: function and dysfunction. Seminars in Immunopathology 31(4): 497—511. https://doi.org/10.1007/s00281-009-0177-0 [published Online First: Epub Date].

[19] Banks, W.A., 2012. Brain meets body: the blood-brain barrier as an endocrine interface. Endocrinology 153(9):4111—4119. https://doi.org/10.1210/en.2012-1435 [published Online First: Epub Date].

[20] Mathiisen, T.M., Lehre, K.P., Danbolt, N.C., Ottersen, O.P., 2010. The perivascular astroglial sheath provides a complete covering of the brain microvessels: an electron microscopic 3D reconstruction. Glia 58(9):1094—1103. https://doi.org/10.1002/glia.20990 [published Online First: Epub Date].

[21] Banks, W.A., Burney, B.O., Robinson, S.M., 2008. Effects of triglycerides, obesity, and starvation on ghrelin transport across the blood-brain barrier. Peptides 29(11):2061—2065. https://doi.org/10.1016/j.peptides.2008.07.001 [published Online First: Epub Date].

[22] Mandi, Y., Ocsovszki, I., Szabo, D., Nagy, Z., Nelson, J., Molnar, J., 1998. Nitric oxide production and MDR expression by human brain endothelial cells. Anticancer Research 18(4C):3049—3052.

[23] Spranger, J., Verma, S., Gohring, I., Bobbert, T., Seifert, J., Sindler, A.L., et al., 2006. Adiponectin does not cross the blood-brain barrier but modifies cytokine expression of brain endothelial cells. Diabetes 55(1):141—147.

[24] Qi, Y., Takahashi, N., Hileman, S.M., Patel, H.R., Berg, A.H., Pajvani, U.B., et al., 2004. Adiponectin acts in the brain to decrease body weight. Nature Medicine 10(5):524—529. https://doi.org/10.1038/nm1029 [published Online First: Epub Date].

[25] Ouchi, N., Kihara, S., Arita, Y., Okamoto, Y., Maeda, K., Kuriyama, H., et al., 2000. Adiponectin, an adipocyte-derived plasma protein, inhibits endothelial NF-kappaB signaling through a cAMP-dependent pathway. Circulation 102(11):1296—1301.

[26] Nakazato, M., Murakami, N., Date, Y., Kojima, M., Matsuo, H., Kangawa, K., et al., 2001. A role for ghrelin in the central regulation of feeding. Nature 409(6817):194—198. https://doi.org/10.1038/35051587 [published Online First: Epub Date].

[27] McCoy, A.N., Crowley, J.C., Haghighian, G., Dean, H.L., Platt, M.L., 2003. Saccade reward signals in posterior cingulate cortex. Neuron 40(5):1031—1040.

[28] Tschop, M., Statnick, M.A., Suter, T.M., Heiman, M.L., 2002. GH-releasing peptide-2 increases fat mass in mice lacking NPY: indication for a crucial mediating role of hypothalamic agouti-related protein. Endocrinology 143(2): 558—568. https://doi.org/10.1210/endo.143.2.8633 [published Online First: Epub Date].

[29] Banks, W.A., Tschop, M., Robinson, S.M., Heiman, M.L., 2002. Extent and direction of ghrelin transport across the blood-brain barrier is determined by its unique primary structure. Journal of Pharmacology and Experimental Therapeutics 302(2):822—827. https://doi.org/10.1124/jpet.102.034827 [published Online First: Epub Date].

[30] Zigman, J.M., Nakano, Y., Coppari, R., Balthasar, N., Marcus, J.N., Lee, C.E., et al., 2005. Mice lacking ghrelin receptors resist the development of diet-induced obesity. Journal of Clinical Investigation 115(12):3564—3572. https://doi.org/10.1172/JCI26002 [published Online First: Epub Date].

[31] Blasberg, R.G., Fenstermacher, J.D., Patlak, C.S., 1983. Transport of alpha-aminoisobutyric acid across brain capillary and cellular membranes. Journal of Cerebral Blood Flow and Metabolism : Official Journal of the International Society of Cerebral Blood Flow and Metabolism 3(1):8—32. https://doi.org/10.1038/jcbfm.1983.2 [published Online First: Epub Date].

[32] Patlak, C.S., Blasberg, R.G., Fenstermacher, J.D., 1983. Graphical evaluation of blood-to-brain transfer constants from multiple-time uptake data. Journal of Cerebral Blood Flow and Metabolism : Official Journal of the International Society of Cerebral Blood Flow and Metabolism 3(1):1—7. https://doi.org/10.1038/jcbfm.1983.1 [published Online First: Epub Date].

[33] Glowinski, J., Iversen, L.L., 1966. Regional studies of catecholamines in the rat brain. I. The disposition of [3H]norepinephrine, [3H]dopamine and [3H]dopa in various regions of the brain. Journal of Neurochemistry 13(8):655—669.

[34] Banks, W.A., Kastin, A.J., Huang, W., Jaspan, J.B., Maness, L.M., 1996. Leptin enters the brain by a saturable system independent of insulin. Peptides 17(2): 305—311.

[35] Banks, W.A., Kastin, A.J., 1998. Differential permeability of the blood-brain barrier to two pancreatic peptides: insulin and amylin. Peptides 19(5):883—889.

[36] Baura, G.D., Foster, D.M., Porte Jr., D., Kahn, S.E., Bergman, R.N., Cobelli, C., et al., 1993. Saturable transport of insulin from plasma into the central nervous system of dogs in vivo. A mechanism for regulated insulin delivery to the brain. Journal of Clinical Investigation 92(4):1824—1830. https://doi.org/10.1172/JCI116773 [published Online First: Epub Date].

[37] Banks, W.A., Jaspan, J.B., Huang, W., Kastin, A.J., 1997. Transport of insulin across the blood-brain barrier: saturability at euglycemic doses of insulin. Peptides 18(9):1423—1429.

[38] Zlokovic, B.V., Jovanovic, S., Miao, W., Samara, S., Verma, S., Farrell, C.L., 2000. Differential regulation of leptin transport by the choroid plexus and blood-brain barrier and high affinity transport systems for entry into hypothalamus and across the blood-cerebrospinal fluid barrier. Endocrinology 141(4):1434—1441. https://doi.org/10.1210/endo.141.4.7435 [published Online First: Epub Date].

[39] Dogrukol-Ak, D., Kumar, V.B., Ryerse, J.S., Farr, S.A., Verma, S., Nonaka, N., et al., 2009. Isolation of peptide transport system-6 from brain endothelial cells: therapeutic effects with antisense inhibition in Alzheimer and stroke models. Journal of Cerebral Blood Flow and Metabolism : Official Journal of the International Society of Cerebral Blood Flow and Metabolism 29(2):411—422. https://doi.org/10.1038/jcbfm.2008.131 [published Online First: Epub Date].

[40] Pan, W., Kastin, A.J., 1999. Entry of EGF into brain is rapid and saturable. Peptides 20(9):1091—1098.

[41] Furness, J.B., Hunne, B., Matsuda, N., Yin, L., Russo, D., Kato, I., et al., 2011. Investigation of the presence of ghrelin in the central nervous system of the rat and mouse. Neuroscience 193:1—9. https://doi.org/10.1016/j.neuroscience.2011.07.063 [published Online First: Epub Date].

[42] Cabral, A., Lopez Soto, E.J., Epelbaum, J., Perello, M., 2017. Is ghrelin synthesized in the central nervous system? International Journal of Molecular Sciences 18(3) https://doi.org/10.3390/ijms18030638 [published Online First: Epub Date].

[43] Cabral, A., De Francesco, P.N., Perello, M., 2015. Brain circuits mediating the orexigenic action of peripheral ghrelin: narrow gates for a vast kingdom. Frontiers in Endocrinology (Lausanne) 6:44. https://doi.org/10.3389/fendo.2015.00044 [published Online First: Epub Date].

[44] Langlet, F., Levin, B.E., Luquet, S., Mazzone, M., Messina, A., Dunn-Meynell, A.A., et al., 2013. Tanycytic VEGF-A boosts blood-hypothalamus barrier plasticity and access of metabolic signals to the arcuate nucleus in

response to fasting. Cell Metabolism 17(4):607–617. https://doi.org/10.1016/j.cmet.2013.03.004 [published Online First: Epub Date].

[45] Schaeffer, M., Langlet, F., Lafont, C., Molino, F., Hodson, D.J., Roux, T., et al., 2013. Rapid sensing of circulating ghrelin by hypothalamic appetite-modifying neurons. Proceedings of the National Academy of Sciences of the U S A 110(4):1512–1517. https://doi.org/10.1073/pnas.1212137110 [published Online First: Epub Date].

[46] Kojima, M., Kangawa, K., 2005. Ghrelin: structure and function. Physiological Reviews 85(2):495–522. https://doi.org/10.1152/physrev.00012.2004 [published Online First: Epub Date].

[47] Beaumont, N.J., Skinner, V.O., Tan, T.M., Ramesh, B.S., Byrne, D.J., MacColl, G.S., et al., 2003. Ghrelin can bind to a species of high density lipoprotein associated with paraoxonase. Journal of Biological Chemistry 278(11):8877–8880. https://doi.org/10.1074/jbc.C200575200 [published Online First: Epub Date].

[48] De Vriese, C., Hacquebard, M., Gregoire, F., Carpentier, Y., Delporte, C., 2007. Ghrelin interacts with human plasma lipoproteins. Endocrinology 148(5): 2355–2362. https://doi.org/10.1210/en.2006-1281 [published Online First: Epub Date].

[49] Tong, J., Dave, N., Mugundu, G.M., Davis, H.W., Gaylinn, B.D., Thorner, M.O., et al., 2013. The pharmacokinetics of acyl, des-acyl, and total ghrelin in healthy human subjects. European Journal of Endocrinology 168(6):821–828. https://doi.org/10.1530/EJE-13-0072 [published Online First: Epub Date].

[50] Cleverdon, E.R., McGovern-Gooch, K.R., Hougland, J.L., 2016. The octanoylated energy regulating hormone ghrelin: an expanded view of ghrelin's biological interactions and avenues for controlling ghrelin signaling. Molecular Membrane Biology 33(6–8):111–124. https://doi.org/10.1080/09687688.2017.1388930 [published Online First: Epub Date].

[51] Diano, S., Farr, S.A., Benoit, S.C., McNay, E.C., da Silva, I., Horvath, B., et al., 2006. Ghrelin controls hippocampal spine synapse density and memory performance. Nature Neuroscience 9(3):381–388. https://doi.org/10.1038/nn1656 [published Online First: Epub Date].

